An Investigation of Grid Resolution on Hypersonic Viscous Flow Simulation

Quanhua Sun[1], Huiyu Zhu[1], Tengfei Su[2]

1 State Key Laboratory of High-temperature Gas Dynamics, Institute of Mechanics, Chinese Academy of Sciences, Beijing, P.R.China, 100190

2 School of Mathematics and Systems Science, Beihang University, Beijing, P.R.China, 100191

(E-mail: qsun@imech.ac.cn)

Abstract The effects of grid resolution on hypersonic viscous flow simulations are investigated in detail. Previous studies have shown that grid plays an important role on the aerothermodynamic predictions for a hypersonic vehicle. We investigate flows over simplified geometry to analyze the behavior of grid resolution when the flow is solved using the Navier-Stokes equations. It shows that grid independent solutions can be achieved with fine meshes where the surface-based cell Reynolds number is in the order of 10. The reason for fine meshes is analyzed using wall functions derived using the boundary layer approximation. It is found that the truncated error of numerical schemes is increased dramatically when the flow approaches the surface, which explains the fact that near-surface cells should be much smaller than faraway cells to maintain the numerical error at a low level.

Key words hypersonic viscous flow, grid resolution, CFD, truncated error

1 Introduction

It is well known that hypersonic flow is challenging for computational fluid dynamics (CFD) to predict its aerothermodynamics because it involves complex physical phenomena and requires large computational resources (Bertin & Cummings, 2006). The grid density is one of key factors that affect the prediction accuracy. Generally, a finer grid produces less spatial discretization error but requires larger computational resources.

In the literature, there have been various studies regarding the requirement of grid density or grid resolution. Papadopoulos et al. (1999) suggest to use the surface-based cell Reynolds number and the temperature jump from the wall to the first cell center to monitor the grid effects. Different values for critical cell Reynolds number have been proposed depending on the numerical scheme and flow problem. It seems that a grid sensitivity study is very important as Men'shov & Nakamura (2000) showed that a small value of order 10 of cell Reynolds number might result in 100% error in the vicinity of the stagnation point. Besides the cell Reynolds number, Chen et al. (2012) proposed that the cell size of the near-wall cells should be in the order of molecular mean free path. However, for many engineering applications, grid-independent solutions may not be practically attainable. Extrapolation techniques such as the Richard extrapolation technique are often adopted to derive the asymptotic solution. The accuracy of the extrapolation depends on the solutions being in the asymptotic grid convergence range.

In this paper, we aim to investigate the behavior of grid resolution on hypersonic viscous flow prediction and to illustrate the cause for fine grid requirement near the wall surface. For this purpose, only simplified geometries are used but general behavior may be applied to similar flow problems.

2 Numerical Observations

We simulate hypersonic flows over simple geometries to illustrate the grid resolution effects. Simulations are performed using our in-house CFD code solving the Navier-Stokes equations. The code employs the MUSCL type finite volume method with

Roe's FDS scheme and the minmod limiter for the convective flux evaluation and the central difference scheme for the viscous flux calculation.

We start with the flow over a front step. The simulated gas is argon, which is preferred for kinetic particle simulation that is adopted for the purpose of validation. Other specification of the case is: step height 2*h*, wall temperature 1000 K, free stream gas temperature 200 K, free stream Mach number 10, free stream Knudsen number (λ/h) 0.001, free stream Reynolds number 13000.

2.1 Grid design

In CFD practices, grid independence studies are usually performed by refining grids with personnel experience or until numerical results agree with experimental or flight data. For simplified geometry we are able to design a systematic series of grids.

For flow over a front step, two sets of grids are designed. One set is equally-spaced grid whose grid size is set at 1/5, 1/10, 1/20, 1/40, 1/80 of the semi-height of the step, respectively. The other set employs clustered grid where the grid near the surface is smoothly refined based on the equally-spaced mesh whose size is 1/80*h*, and the smallest mesh size in the normal direction is set as 1/2, 1/4, 1/8, 1/16, 1/32, 1/64, 1/128 of the base mesh size, respectively.

2.2 Hypersonic flow over a front step

The hypersonic flow over a front step is illustrated in Fig. 1 where the temperature field $(T-T_\infty)/(T_{shock}-T_\infty)$ is plotted. Simulations (Fig. 2) show that the shock location can be captured correctly even with a coarse mesh having the size of 1/80*h* only that the shock thickness is affected. Figure 3 shows the surface properties predicted using different grid resolution. It seems that the grid resolution has little effect on the surface pressure but affects strongly the values of skin friction and heat flux. Particularly we plot the

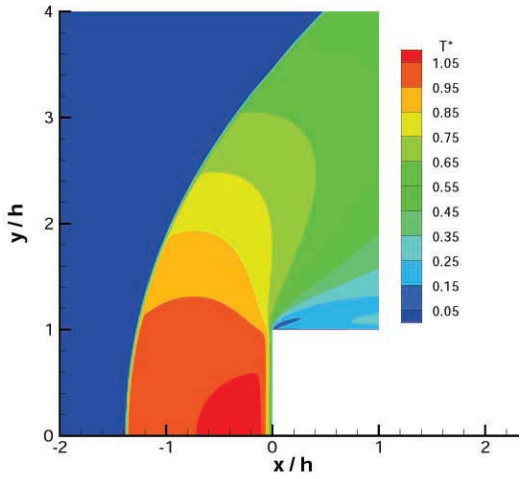

Figure 1 Temperature field of argon flow over a front step

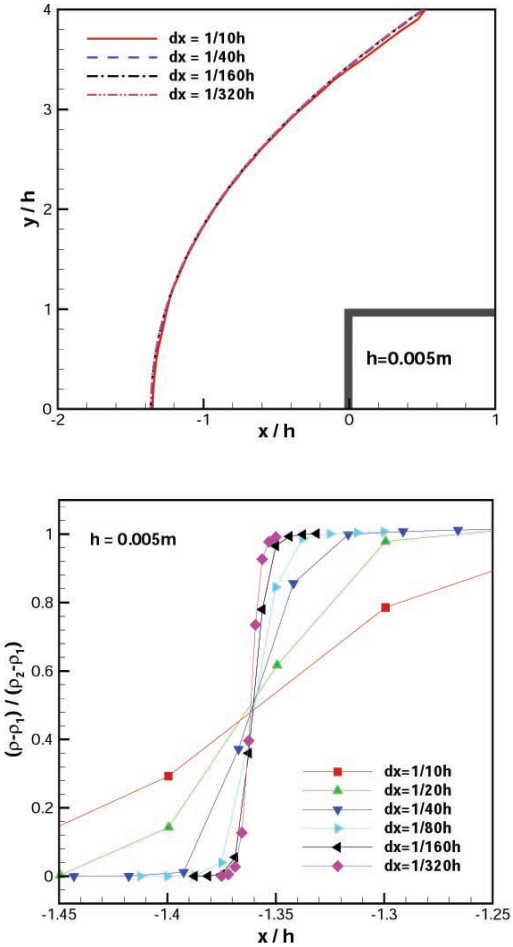

Figure 2 Predicted shock profile for flow over a front step

predicted heat flux coefficient on surface located at 0.5 *h* height where *dx* is the smallest grid size (Fig. 4). The predicted heat flux increases quickly with grid refinement at early stage. After it reaches its maximum, the value converges gradually to a constant that is the

grid-independent value. This behavior also applies to the skin friction. For the present case, a grid size around 1/1000 of the semi step height is needed to reach the grid-independent value. This accurate value may be encountered using a much larger cell size, which is a pure luck. The non-monotonic feature also makes extrapolation techniques difficult to apply.

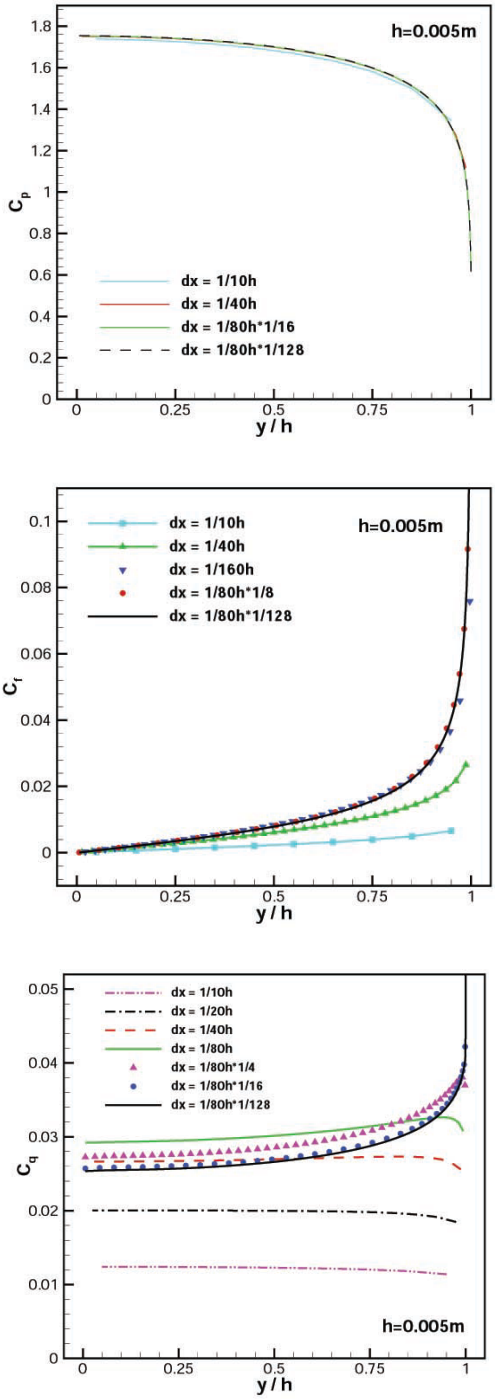

Figure 3 Predicted surface properties (pressure, skin friction, heating) for flow over a front step

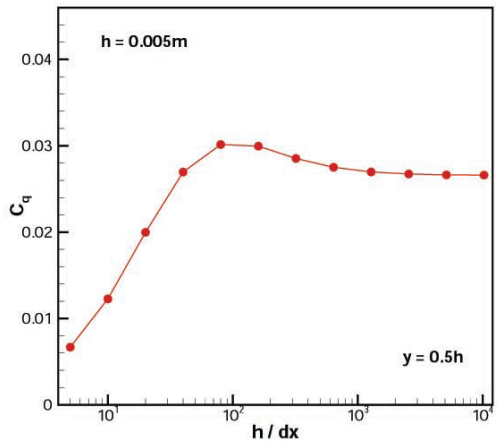

Figure 4 Predicted heat flux coefficient at 0.5 *h* height for flow over a front step

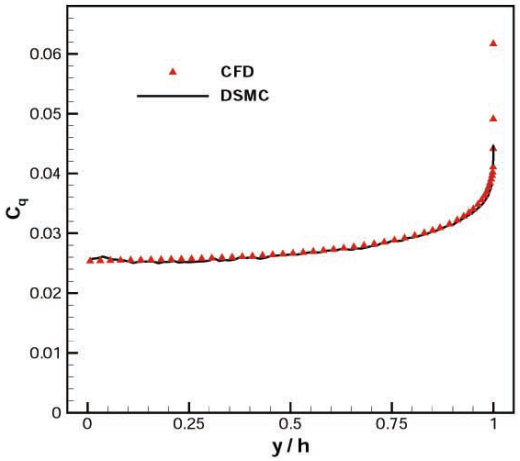

Figure 5 Comparison of heat flux coefficient obtained using CFD and DSMC for flow over a front step

It is necessary to validate whether the converged heat flux is the physical solution of the flow. The direct simulation Monte Carlo (DSMC) method is employed to simulate the same flow. Figure 5 shows that the overall agreement between DSMC and CFD solutions is satisfactory. Difference is observed only in a very small region near the step corner, which can be attributed to two factors. One is that it is hard for CFD to capture the flow gradients near the corner. Another is that the local Knudsen number near the corner is large and the Navier-Stokes equations become invalid in this small region. Therefore, it can be concluded that the grid-independent result is the physical solution of the Navier-Stokes equations.

2.3 Other cases

The behavior of grid resolution effects in Fig. 4 is observed in other similar cases. Figure 6 presents CFD results for several problems including flow over front-step, cylinder, and sphere under different flow conditions. The simulated gases are argon and air. In the plot, the mesh size is represented by the surface-based cell Reynolds number. It shows that mesh-independent results are obtained for all the cases when Re_g is less than 5. Of course, many factors will affect the behavior of grid independence. For instance, different numerical scheme will have slight different converging process of grid resolution as shown in Fig. 7 where the flow over a cylinder is simulated.

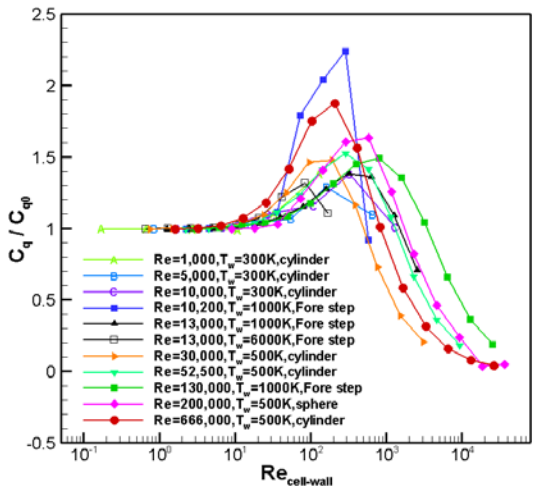

Figure 6 Effects of surface-based cell Reynolds number on heat flux predicted at the stagnation point

Surface-based cell Reynolds number specifies the size of cells near surface. Cell clustering will also affect the prediction accuracy. In practice, larger cells are used in domain away from the surface in order to save computational cost. Then the flow may not be resolved locally using the large cells. In addition, the non-uniform grid will produce additional numerical error. This may be the reason why grids having very small surface cells may predict bad results sometime. Figure 8 shows that obvious numerical error will occur when the size ratio between neighboring cells is larger than 1.2.

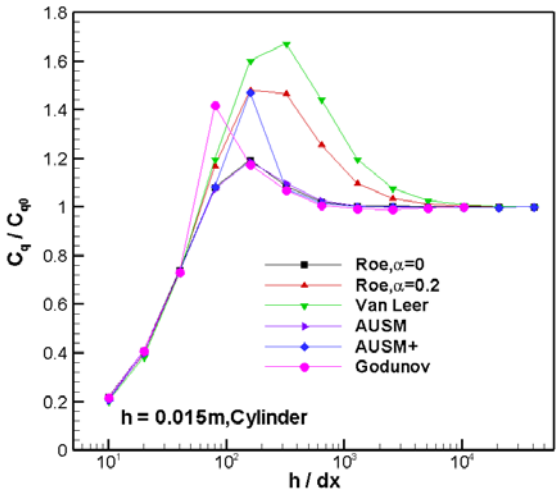

Figure 7 Heat flux coefficient predicted by numerical schemes for flow over a cylinder. Schemes employed are: Roe's FDS scheme, Roe's scheme with entropy fix, van Leer's FVS scheme, AUSM scheme, AUSM+ scheme, and exact Riemann (Godunov) solver.

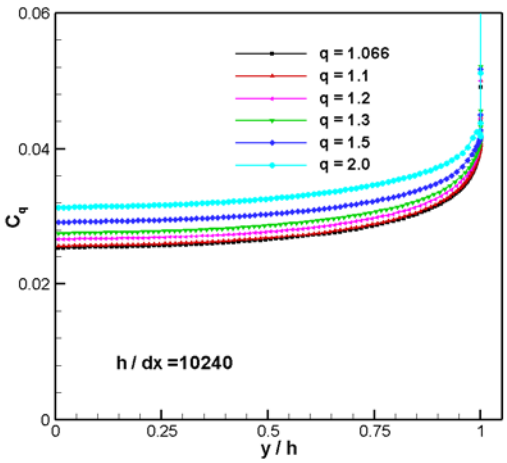

Figure 8 Effects of surface-based cell Reynolds number on heat flux predicted at the stagnation point

3 Theoretical Analysis

From numerical observation, it is clear that the cell size should be small near the surface to predict correctly the surface properties. The main reason may be that the gradients of flow properties are large in the boundary layer. To analyze the flow near the surface, we derive the wall functions for velocity and temperature, and investigate the scheme error in this smooth flow region.

3.1 Wall function

For hypersonic laminar flow, we can derive wall functions for flow properties within the boundary layer where the quasi-one-dimensional flow can be assumed. These functions are derived using the cell values as follows (Zhu 2012):

$$T(y) = T_w (cy+1)^{\frac{1}{\omega+1}} \tag{1}$$

$$u(y) = \frac{\omega+1}{dx}\left(c_3 y+1\right)^{\frac{1}{\omega+1}}\left(Dy+Ey^2+F\right) \tag{2}$$

$$v(y) = (\omega+1)\frac{b}{c}\frac{T}{T_w}\left(\frac{1}{c}\frac{\omega+1}{\omega+2}\left(\frac{T}{T_w}\right)^{\omega+1} - y\right) + (\omega+1)\frac{a}{c}\left(\frac{T}{T_w}-1\right) - \frac{b}{c^2}\frac{(\omega+1)^2}{\omega+2} \tag{3}$$

where ω is the power index in viscosity ($\mu \sim T^{\omega}$), and

$$c = \frac{1}{y_c}\left(\left(\frac{T_c}{T_w}\right)^{\omega+1} - 1\right),$$

$$b = -\frac{1}{\mu_w}\frac{dp}{dx},$$

$$a = \frac{cu_c + \frac{b}{c}\frac{(\omega+1)^2}{\omega+2} - A}{(\omega+1)\left(T_c/T_w - 1\right)},$$

$$A = b(\omega+1)\frac{T_c}{T_w}\left(\frac{\omega+1}{\omega+2}\frac{1}{c}\left(\frac{T_c}{T_w}\right)^{\omega+1} - y_c\right),$$

$$D = \frac{a_4 p_4}{c_4 p_3} - \frac{a_2 p_2}{c_2 p_3} + \frac{\omega+1}{\omega+2}\left(\frac{b_4 p_4}{p_3 c_4^2} - \frac{b_2 p_2}{p_3 c_2^2}\right),$$

$$E = -\frac{0.5}{\omega+2}\left(\frac{p_4 b_4}{p_3 c_4} - \frac{p_2 b_2}{p_3 c_2}\right),$$

$$F = \frac{\omega+1}{\omega(\omega+2)}(G-H),$$

$$G = \frac{p_2}{p_3}\frac{a_2 c_2(\omega+2) + b_2(\omega+1)}{c_2^3}\left(\left(c_2 y+1\right)^{\frac{\omega}{\omega+1}} - 1\right),$$

$$H = \frac{p_4}{p_3}\frac{a_4 c_4(\omega+2) + b_4(\omega+1)}{c_4^3}\left(\left(c_4 y+1\right)^{\frac{\omega}{\omega+1}} - 1\right).$$

y_c is the cell center location, and the subscripts 1-4 refer to four faces as shown in Fig. 9. The wall functions describe the distributions from surface to the cell center. Notice that information from three cells is required to obtain u which is driven by the tangent pressure gradient.

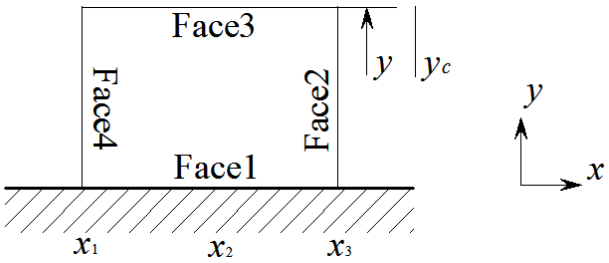

Figure 9 Geometry for a surface cell

The accuracy of wall functions is found to be very good where the boundary layer approximation is satisfied. Figure 10 shows the comparison of the temperature and normal velocity distributions at the location of 0.5 *h* height with the values obtained between reference CFD with very fine grid and wall functions. Using the wall functions, the flow within the boundary layer is now described in explicit functions, which allows us to analyze the scheme error.

The wall functions can also be used to calculate the flow gradients on the surface, thus the boundary conditions at surface can be correctly evaluated. For instance, the surface heat transfer is evaluated as

$$q = \mu_w \cdot \frac{1}{\omega+1}\frac{\left(T_c/T_w\right)^{\omega+1} - 1}{T_c/T_w - 1}\cdot\frac{T_c - T_w}{y_c}.$$

This boundary condition has been implemented in our in-house code. The improvement on the heating prediction is quite limited, however, which may indicated that the cell size requirement does not come from the boundary implementation.

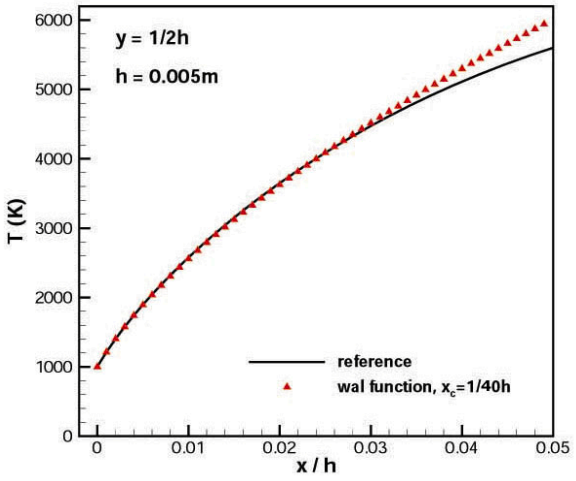

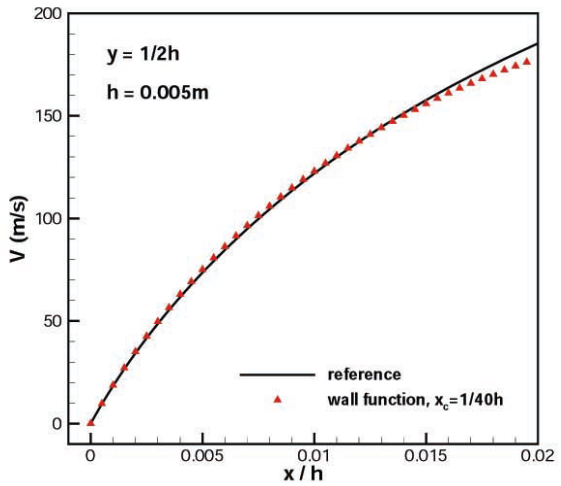

Figure 10 Comparison of flow properties near the surface between reference CFD data and wall function prediction

3.2 Truncated error from numerical scheme

The equivalent differential equation of a MUSCL type scheme can be analyzed in the smooth flow region using Taylor expansions.

Here we derive the truncated error from the x-component discretization for a 2nd order limiter. Namely,

$$\frac{F_{i+1/2}-F_{i-1/2}}{\Delta x}=\frac{\partial F}{\partial x}+\alpha\Delta x^2+O\left(\Delta x^3\right). \quad (4)$$

For two-dimensional simulation and with van leer limiter $\varphi(R)=\frac{2R}{R+1}$, we have the coefficients derived for the 2nd order term as,

$$\alpha_1=-\frac{1}{12}\frac{\partial^3\rho u}{\partial x^3}$$

$$\alpha_2=\frac{\gamma-1}{24}\left(3\frac{\partial\rho}{\partial x}\frac{\partial v}{\partial x}\frac{\partial v}{\partial x}+2v\frac{\partial^3\rho v}{\partial x^3}-v^2\frac{\partial^3\rho}{\partial x^3}-2\frac{\partial^3\rho E}{\partial x^3}\right)+\frac{\gamma-3}{24}\left(3\frac{\partial\rho}{\partial x}\frac{\partial u}{\partial x}\frac{\partial u}{\partial x}+2u\frac{\partial^3\rho u}{\partial x^3}-u^2\frac{\partial^3\rho}{\partial x^3}\right)$$

$$\alpha_3=\frac{1}{12}\left(uv\frac{\partial^3\rho}{\partial x^3}-v\frac{\partial^3\rho u}{\partial x^3}-u\frac{\partial^3\rho v}{\partial x^3}-3\frac{\partial\rho}{\partial x}\frac{\partial u}{\partial x}\frac{\partial v}{\partial x}\right)$$

$$\alpha_4=\frac{1-\gamma}{8}\left(\left(\rho\frac{\partial u}{\partial x}-\mathrm{u}\frac{\partial\rho}{\partial x}\right)\left(\frac{\partial u}{\partial x}\frac{\partial u}{\partial x}+\frac{\partial v}{\partial x}\frac{\partial v}{\partial x}\right)\right)-\frac{1-\gamma}{8}\frac{\partial\rho}{\partial x}\frac{\partial u}{\partial x}\frac{\partial\left(u^2+v^2\right)}{\partial x}+\frac{1-\gamma}{12}\mathrm{u}\left(u^2+v^2\right)\frac{\partial^3\rho}{\partial x^3}+\frac{1-\gamma}{24}\left(-\left(3u^2+v^2\right)\frac{\partial^3\rho u}{\partial x^3}-2uv\frac{\partial^3\rho v}{\partial x^3}\right)+\frac{\gamma}{12}\left(uE\frac{\partial^3\rho}{\partial x^3}-u\frac{\partial^3\rho E}{\partial x^3}-E\frac{\partial^3\rho u}{\partial x^3}-3\frac{\partial\rho}{\partial x}\frac{\partial u}{\partial x}\frac{\partial E}{\partial x}\right)$$

The values of these coefficients vary within the flow field. If the wall functions are used to describe the flow, we can evaluate the values for these coefficients in the near surface region, which is plotted in Fig. 11. It seems that the truncated error of the scheme increases about 100 times from the cell center to the surface, which is quite amazing. If the same truncated error is desired, then the cell size should differ by 10 times. This explains the fact that near-surface cells should be much smaller than faraway cells in many CFD practices.

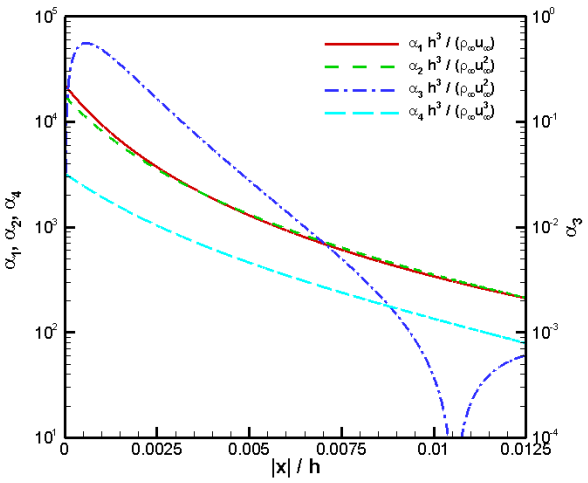

Figure 11 Truncated error of the scheme at 0.5 *h* height for flow over a front step

4 Concluding Remarks

The mesh resolution plays a very important role on prediction of hypersonic aerothermodynamics. In order to obtain grid-independent solutions, the surface-based cell Reynolds number should be less than 10. Otherwise, the skin friction and surface heating can be predicted either too large or too small. The requirement for this cell restriction comes from pure numerical issue as the truncated error of the discretized scheme varies a lot within the boundary layer. Higher-order schemes are therefore required to avoid employment of very fine grids.

Acknowledgement

This work was supported by the National Natural Science Foundation of China through grants 11372325 and 91116013.

References

[1] Bertin, J.J. & Cummings, R. M., Critical Hypersonic Aerothermodynamic Phenomena [J], Annual Review of Fluid Mechanics, 2006, 38, 129-157.

[2] Papadopoulos, P., Venkatapathy, E., Prabhu, D., Loomis, M.P. & Olynick, D., Current Grid-generation Strategies and Future Requirements in Hypersonic Vehicle Design, Analysis, and Testing, Appl. Math. Model, 23, 705-735, 1999.

[3] Men'shov, I.S. & Nakamura, Y., Numerical Simulations and Experimental Comparison for High-speed Nonequilibrium Air Flows, Fluid Dyn. Res., 27, 305-334, 2000.

[4] Chen, X. Ai, B. & Wang, Q., A Wall Grid Scale Criterion Based on the Molecular Mean Free path for the Wall Heat Flux Computations by the Navier-Stokes Equations (in Chinese), Chinese Journal of Theoretical and Applied Mechanics, 42(6), 1083-1089, 2010.

[5] Bird, G.A., Molecular Gas Dynamics and the Direct Simulation of Gas Flow, Clarendon Press, 1994.

[6] Zhu, H., Numerical Study of Hypersonic Aerodynamics Characteristics in Hypersonic Flow Based on Grid Effects, PhD Dissertation. Chinese Academy of Sciences, 2012.